Hindawi
Geofluids
Volume 2023, Article ID 1576401, 14 pages
https://doi.org/10.1155/2023/1576401

Research Article

Identifying Effective Rock-Breaking Ratio Based on Rock Chip Information for Rock-Breaking Efficiency Evaluation of TBM

Chuigang Zeng,[1] Changbin Yan,[2] Gaoliu Li,[2] Xiao Xu,[3] Fengwei Yang,[4] and Weilin Su[4]

[1]*State Key Laboratory of Shield Machine and Boring Technology, Zhengzhou, Henan 450001, China*
[2]*School of Civil Engineering, Zhengzhou University, Zhengzhou, Henan 450001, China*
[3]*School of Resources and Safety Engineering, Central South University, Changsha, Hunan 410083, China*
[4]*Yellow River Engineering Consulting Co., Ltd., Zhengzhou, Henan 450003, China*

Correspondence should be addressed to Xiao Xu; xiaoxu@csu.edu.cn

Received 20 July 2022; Revised 13 September 2022; Accepted 1 October 2022; Published 25 October 2023

Academic Editor: Jinpeng Zhang

The rock chip information (shape, size, and particle size distribution) could comprehensively reflect the characteristics of rock mass and rock-breaking efficiency of TBM. This study is aimed at defining a novel index (effective rock-breaking ratio, P_r) to identify the rock-breaking efficiency of TBM based on the rock chip information. To evaluate this approach, a series of field sieving and measuring tests of rock chips was conducted at the water conveyance tunnel construction projects of China. The rock-breaking efficiency evaluation and tunneling parameter improvement of TBM were researched based on P_r index. The results showed as follows: (1) from the perspective of energy conversion, the rock chip surface area was calculated through the rock chip cumulative volume distribution model. P_r is used to evaluate the rock-breaking efficiency of TBM based on the proportion of surface area of rock chips with particle size larger than 5 mm; (2) P_r has a good linear correlation with coarseness index (CI) and specific energy (SE), the higher the TBM tunneling efficiency, the larger P_r and CI values, the less SE values; (3) P_r increases at first and then decreases with the rise of thrust force of TBM. The optimal thrust force intervals for grade II and III surrounding rocks can be determined to improve the rock-breaking efficiency of TBM. Findings from this study are insightful in terms of accurately evaluating the excavation efficiency and improving the tunneling parameters of TBM.

1. Introduction

Tunnel boring machine (TBM) is the most effective construction method of tunnel excavation; its core competitiveness lies in the high achieved construction speed [1–7]. Therefore, with the premise of ensuring safety while reducing tool wear, it is crucial to enhance the rock-breaking efficiency of TBM [8].

The potential factors influencing the rock-breaking efficiency of TBM include rock compressive strength, tensile strength, confining pressure, joint development, TBM equipment performance, cutter spacing, and tunneling parameters [9–20]. Rock chips in TBM are formed by the disc cutters cutting the rock palm surface. According to the rock fragmentation theory [21], the rock-breaking effect of TBM disc cutters is achieved by a mixed action of the tensile failure, crushing failure, and shearing failure of rock mass [22, 23]. The rock chip information can directly reflect the "rock-machine" interaction mechanism, identify the quality of surrounding rock and the geology in TBM construction, and indirectly reflect the mechanical properties and tunneling parameters of TBM [24]. Therefore, the rock chip information is closely related to the characteristics of the surrounding rock, the mechanical energy utilization rate, and the rock-breaking efficiency of TBM [14, 20, 25–27].

Tuncdemir et al. [27] and Gong et al. [28] experimentally put forward that the coarseness index [29] of rock chips is an effective indicator of the rock-breaking efficiency of TBM. However, the rock chips with larger particle size are repeatedly calculated in the calculation of coarseness index. Specific energy is considered as a valid parameter evaluating the efficiency of TBM [7, 30, 31]. Nevertheless, the specific energy value calculated in the construction process of TBM varies greatly, which lead to the deviation between calculated specific energy value and actual specific energy value. Heydari et al. [14], Mohammadi et al. [32], and Kumar et al. [33] provided the correlation between the particle size distribution of rock chips and the rock-breaking method, namely, the tunneling parameters.

TBM transforms mechanical energy into surface energy and increases the free surface in the process of rock breaking [21]. The higher the degree of rock fragmentation, the larger the total surface area of rock chips, and the more work the machine performs. The rock chip volume of a certain particle size is proportional to the total surface area when the tunnel section is certain [29]. The total surface area of rock chips can reflect the energy absorbed when the rock mass is broken into rock chips. The overall quality of rock chips collected in each sieving test is different. Thus, the surface area of each group of rock chips cannot be directly used to assess the rock-breaking efficiency of TBM. Likewise, the specific surface area of rock chips is not suitable for evaluating the efficiency of TBM, because the index cannot emphasize the content of rock chips with large size. However, no specific parameter has been proposed for quantitatively assessing the rock-breaking efficiency of TBM. Little is known about the correlation between the size and slice shape of rock chips formed by the cutters and the specific energy or the rock-breaking efficiency during TBM tunneling [28, 32, 34]. Therefore, despite previous reports on the correlation between rock chip parameters and the rock-breaking efficiency of TBM [14, 28], a systematic investigation of the new index to assess the rock-breaking efficiency of TBM based on the rock chip information is of great value.

This work is aimed at experimentally identifying P_r to assess the rock-breaking efficiency of TBM based on the shape, size, and particle size distribution of rock chips. The rock chips were collected from Lanzhou water conveyance tunnel construction project and Wananxi water diversion project, China, and a series of field sieving and measuring tests was conducted. The calculation method of P_r index was formulated based on the total surface area. The internal correlations among P_r, CI, SE, and the tunneling parameters were investigated.

2. Project Background and Field Sieving Tests

2.1. Lanzhou Water Conveyance Tunnel Construction Project. The water conveyance project consists of water tunnels, branch lines, plants, and municipal pipelines. The main water conveyance tunnel connects the Lijiaxia Reservoir and the Lujiaping water treatment plant and is 31.57 km long (as shown in Figure 1). The tunnel was constructed using two double-shield TBMs started drilling from the two ends of the water conveyance tunnel. TBM 1 started from the Lijiaxia Reservoir side, and TBM 2 started from the Lujiaping water treatment plant side. The two sections of the main tunnel were named TBM 1 and 2, and their lengths were 12.227 km and 13.259 km, respectively. The longitudinal gradient of the main tunnel is about 0.1%. The excavation diameter of the main tunnel was initially designed as 5.46 m and measured as 4.60 m after construction. The maximum buried depth of the main tunnel is 918 m.

The geological profile along the water conveyance tunnel is shown in Figure 2. The water conveyance tunnel passes through five different lithologies of different geological formations, including quartz diorite of middle Caledonian ($\delta o_3{}^2$), hornblende quartz schist of pre-Sinian Maxianshan Group ($AnZmx^4$), granite of mid-Caledonian ($\gamma_3{}^2$), interbedded mudstone and siltstone of Lower Cretaceous Hekou Group (K_1hk^1), and metamorphic andesite of Ordovician Upper Middle Wusu Mountain Group ($O_{2\text{-}3}wx^2$). Detailed field surveys were conducted to investigate the rock mass quality of the five lithologies in the study area, and some rock characteristics are summarized in Table 1. The main design parameters of the double-shield TBM are also collected and summarized in Table 2.

2.2. Wananxi Water Diversion Project. Wananxi water diversion project consists of water intake buildings, diversion tunnels, and pipelines. The main water conveyance tunnel connects the Manzhu River and Beiyi water treatment plant and is 34.31 km long (as shown in Figure 3). The tunnel was constructed with the combination of drilling and blasting method, TBM method, and buried pipe method, and their lengths were 13.346 km, 14.001 km, and 6.077 km, respectively. The pressurized tunnel is used in the whole process of water delivery line to convey water. The downstream pressure tunnel is to be constructed by the open TBM with a circle excavation section of 3.83 m in diameter.

The geological profile along the water conveyance tunnel is shown in Figure 4. The water conveyance tunnel passes through three different lithologies of different geological formations, including granite of early Yanshanian ($\gamma_5{}^{2(3)c}$), diorite of early Yanshanian ($\gamma\delta_5{}^{2(3)b}$), and quartz sandy conglomerate of sedimentary basin (D_3t^a). Detailed field surveys were conducted to investigate the rock mass quality of the three lithologies in the study area, and some rock characteristics are summarized in Table 3. The main design parameters of open-type TBM are summarized in Table 2.

2.3. Field Sieving Test of Rock Chips. The rock chip information during TBM tunneling is an indirect factor for the evaluation of surrounding rock quality and rock-breaking efficiency of TBM [27]. Due to the complex interplay of engineering geological conditions, rock-breaking behavior of TBM cutters, cutter arrangement, and tunneling parameters, the rock chips generated by TBM tunneling exhibit some randomness. Therefore, it is significant to evaluate the rock-breaking efficiency and optimize the tunneling parameters of TBM based on rock chip information. Field sieving and measuring tests are widely used measure of rock chip information because of its simple operation and robust accuracy.

To obtain the shape, size, and particle size distribution regularity information of rock chips, 12 groups of field sieving tests of rock chips for different lithologies were conducted in Lanzhou water conveyance tunnel construction project and Wananxi water diversion project (as shown in Figure 5). All rock specimens were divided into hard rock and soft rock according to the Code for Engineering

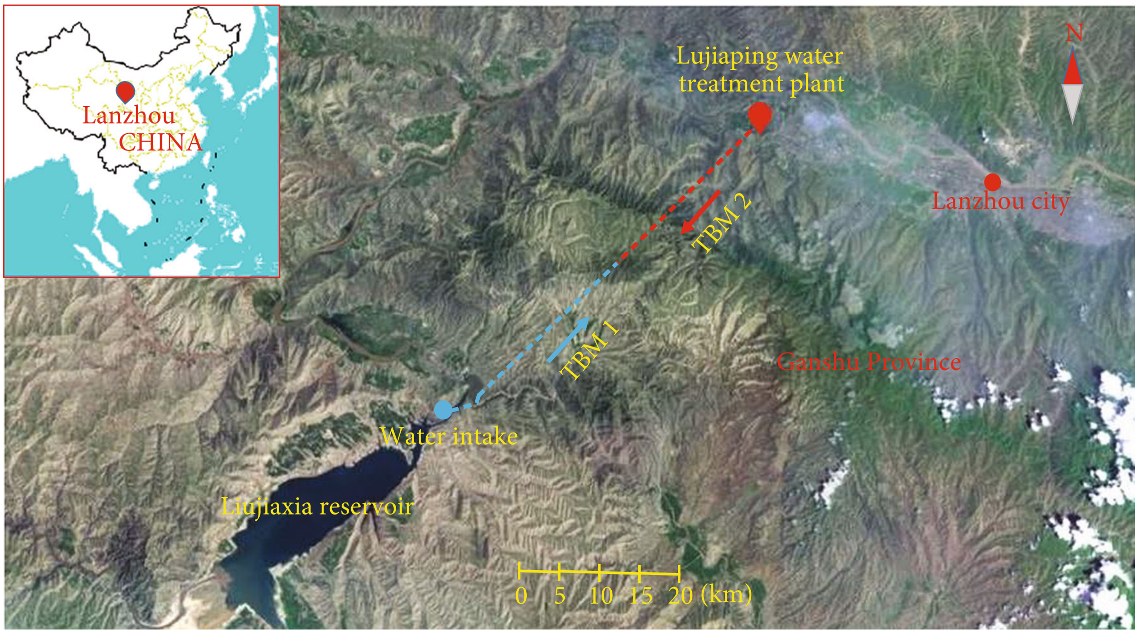

Figure 1: Construction layout of Lanzhou water conveyance tunnel construction project.

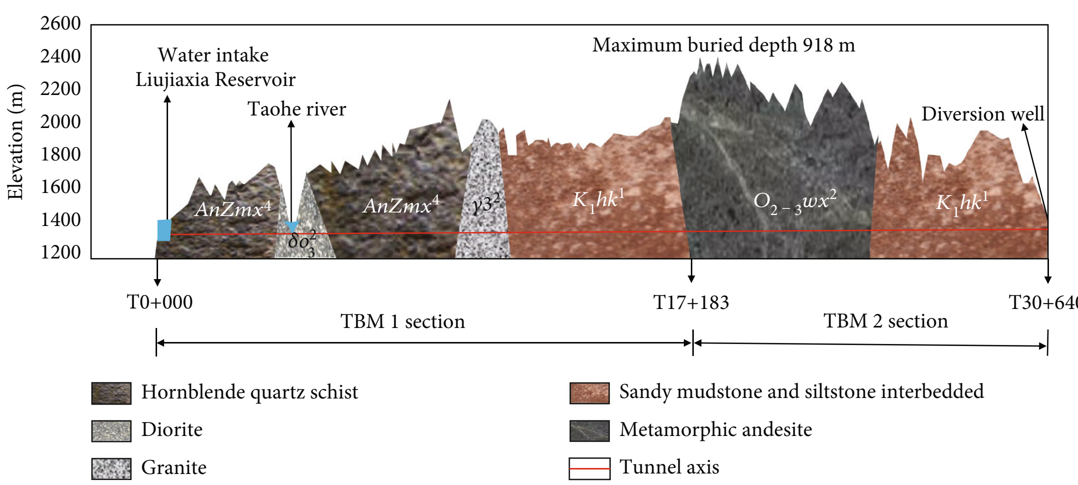

Figure 2: Geological profile of Lanzhou water conveyance tunnel construction project.

Geological Investigation of Water Resources and Hydropower [35]; the integrity grade of surrounding rock was divided into II and III following the Standard for Engineering Classification of Rock Masses [36], as shown in Table 4. The rock chip specimens were stochastically collected with different tunneling distances from the outlet of the TBM conveyor belt. The rock chips were weighed, and the density of different rocks was measured (as shown in Table 4). The diameters of the standard square-hole sieve were 40 mm, 31.5 mm, 25 mm, 16 mm, 10 mm, 5 mm, and 2.5 mm (7 levels in total).

3. Effective Rock-Breaking Ratio Index

3.1. Rock Chip Cumulative Volume Distribution Model. The cumulative probability analysis and sieving data fitting analysis are two commonly used theoretical methods to investigate the particle size distribution of rock chips. The gradation curves can be obtained by the former, which identifies the overall distribution regularity of particle size. The latter one can evaluate whether the particle size distribution satisfies the theoretical distribution model. Among the distribution functions of the rock chip particle size, the Rosin-Rammler model, the Gandin-Schuhmann model, and the lognormal distribution model are the most widely used ones. The Rosin-Rammler distribution function can assess the particle size distribution of rock chips better in blasting excavation and TBM tunneling [37]. But the quantitative distribution characteristics of rock chips are hard to be obtained by the previously proposed models.

To obtain the distribution regularity of rock chips, the field sieving and measuring tests were conducted. In order to acquire the quantitative distribution characteristic of rock

Table 1: Surrounding rock information of Lanzhou water conveyance tunnel construction project.

Formation	Lithology	Color	Hardness	Weathering resistance	Integrity	Figure
Middle Caledonian ($\delta o_3^{\ 2}$)	Quartz diorite	Gray-black	Hard	Strong	Good	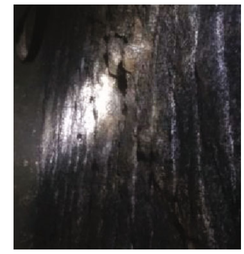
Pre-Sinian Maxianshan Group (AnZmx^4)	Quartz schist	Gray-black and greyish-green	Hard	Strong	Good	
Mid-Caledonian ($\gamma_3^{\ 2}$)	Granite	Off-white	Hard	Strong	Good	
Lower Cretaceous Hekou Group (K$_1$hk^1)	Mudstone and siltstone interbedded	Brown red	Soft	Weak	Poor	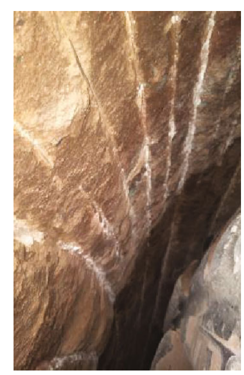
Ordovician Upper Middle Wusu Mountain Group (O$_{2\text{-}3}$wx^2)	Metamorphic andesite	Gray-green	Hard	Weak	Poor	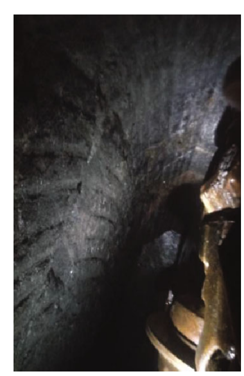

chips, the rock chip cumulative volume distribution model was developed to indirectly obtain the quantitative characteristic of rock chips by referring to the Rosin-Rammler model and Weibull model. The volume of rock chips with particle size larger than each square-hole sieve diameter was calculated, and the cumulative volume of rock chips with larger than the square-hole sieve diameter was also calculated. The correlation between the cumulative volume and cube of particle size of rock chips for different lithologies was investigated (as shown in the following equation and Figure 6).

$$L\left(D^3\right) = a + b\left(1 - \exp^{-\left(D^3 + c\right)/d}\right), \quad (1)$$

Table 2: TBM design parameters for water conveyance tunnel construction projects.

Design parameters	Lanzhou water source construction tunnel project TBM 1	TBM 2	Wananxi water diversion project TBM
Excavation diameter (mm)	5480	5480	3830
TBM type	Double shield		Open
Number of disc cutters	37	30	23
Center disc cutter/diameter (mm)	6/432	4/432	4/432
Inner cutter/diameter (mm)	21/483	17/483	11/432
Gauge cuter/diameter (mm)	19/483	9/483	8/432
Maximum cutterhead spacing (mm)	86	83	89
Cutterhead speed (r·min^{-1})	0~10.3	0~8.7	0~15.8
Cutterhead power (kW)	1800	2100	1200
Maximum cutterhead thrust (kN)	22160	11900	8972
Rating torque (kN·m)	3458	4210	1386
Breakaway torque (kN·m)	5878	6940	2287
Maximum tunneling speed (mm·min^{-1})	120	120	120

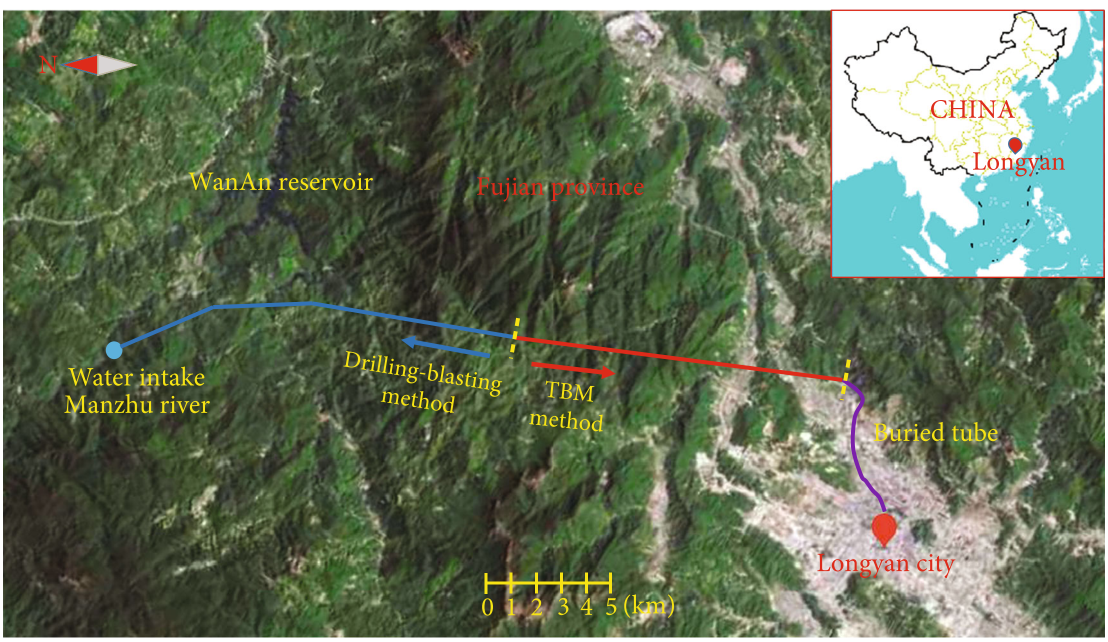

Figure 3: Construction layout of the Wananxi water diversion project.

where $L(D^3)$ represents the cumulative volume of rock chips larger than the particle size (cm^3); a, b, c, and d are the model parameters; and D is the particle size of rock chip (cm).

Figure 6 shows that the rock chip cumulative volume decreases exponentially with the rise cubic of rock chip particle size. The values of R^2 for all exponential regression results are larger than 0.69, which indicates that the correlation between rock chip cumulative volume and cube of rock chip particle size is good. The absolute value of model function derivative could effectively reflect the quantitative distribution of rock chips.

3.2. Surface Area Based on the Rock Chip Distribution Regularity Model. The geometry of rock chips is still a valid index for assessing the rock-breaking mechanical energy of TBM [14, 38]. According to the results of the field sieving and measuring tests, the shape of rock chips with smaller than 0.5 cm particle size is close to a cube, while that of particle sizes equal to and greater than 0.5 cm is close to an ellipsoid.

Therefore, when the particle size of rock chips is less than 0.5 cm, the surface area S_i of a single particle is approximated as follows:

$$S_i = 6D^2. \quad (2)$$

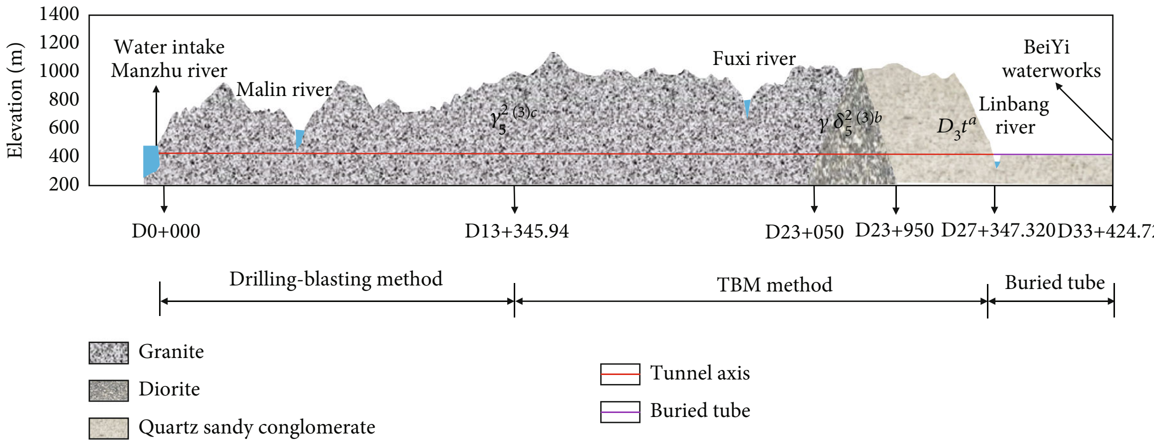

Figure 4: Geological profile of Wananxi water diversion project.

Table 3: Surrounding rock information of Wananxi water diversion project.

Formation	Lithology	Color	Hardness	Weathering resistance	Integrity	Figure
Early Yanshanian ($\gamma_5^{2(3)c}$)	Granite	Gray-black	Hard	Strong	Good	
Early Yanshanian ($\gamma\delta_5^{2(3)b}$)	Diorite	Gray-white	Hard	Strong	Good	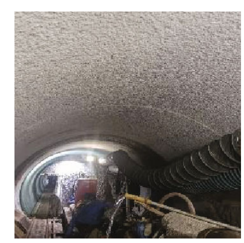
Sedimentary basin (D_3t^a)	Quartz sandy conglomerate	Gray-white and yellow-white	Hard	Strong	Good	

When the particle size of rock chips is ≥0.5 cm, the surface area S_i of a single particle is approximated as follows:

$$S_i = \frac{1}{3}\pi(jq + qt + jt), \tag{3}$$

where j represents the major axis of the ellipsoid (cm), q represents the medium axis of the ellipsoid (cm, $q = D$), and t represents the minor axis of the ellipsoid (cm).

Existing literature investigated the grain size distribution regularity of rock chips [38, 39]. According to the field measuring test results of rock chips, the ratios of major axis to medium axis and minor axis are shown in Table 5.

The total surface area S_T of rock chips for a tunneling section of TBM is calculated as follows:

$$S_T = \sum_{i=0}^{i=D_{\max}} S_i = \int_0^{0.5} S_i\left(-L'\left(D^3\right)\right)dD + \int_{0.5}^{D_{\max}} S_i\left(-L'\left(D^3\right)\right)dD, \tag{4}$$

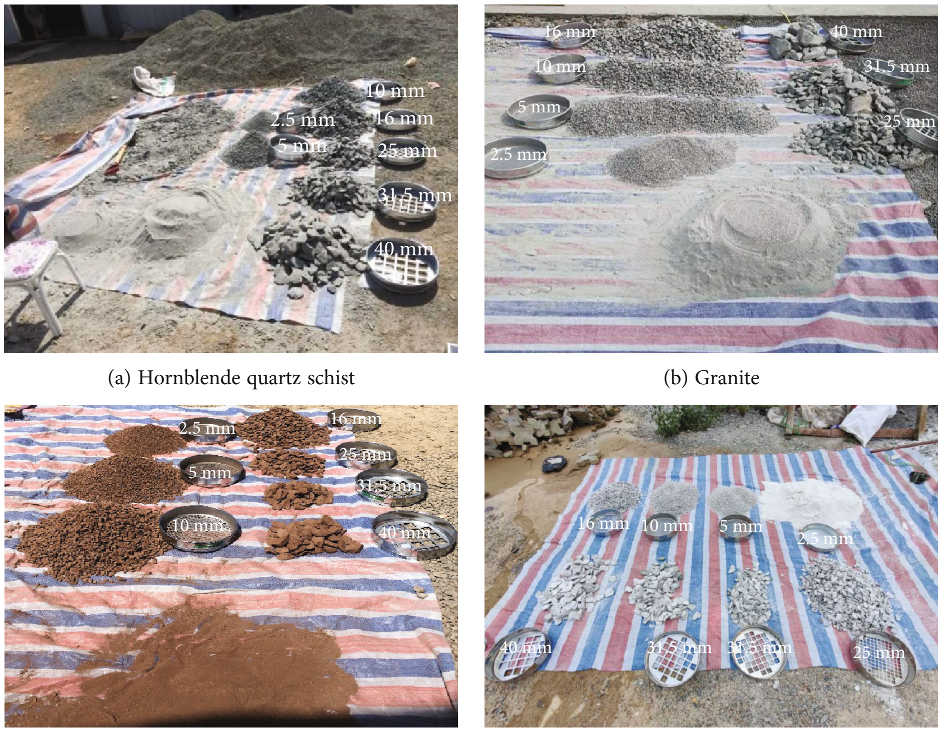

(a) Hornblende quartz schist

(b) Granite

(c) Sandy mudstone and siltstone interbedded

(d) Quartz sandy conglomerate

Figure 5: Sieving tests of rock chips for different lithologies.

Table 4: Sieving test results of rock chips for different lithologies.

Group	Project	Lithology	Tunneling distance (m)	Sieving weight (kg)	Density (g/cm^3)	Hardness	Surrounding rock integrity grade
1	Lanzhou TBM 1	Hornblende quartz schist	16.700	263.165	2.82	Hard	II
2			21.100	212.736			
3			31.500	175.072			
4		Granite	19.600	239.250	2.80		
5			13.500	214.140			
6	Lanzhou TBM 2	Sandy mudstone and siltstone interbedded	17.600	215.173	2.54	Soft	III
7			5.700	164.302			
8			25.533	119.761			
9			24.013	74.604			
10			22.075	194.366			
11	Wananxi TBM	Quartz sandy conglomerate	4.850	180.500	2.68	Hard	II
12			13.610	174.300			

where D_{max} represents the maximum medium axis of rock chips (cm).

3.3. Effective Rock-Breaking Ratio. Based on the energy dissipation theory, the optimal energy conversion ratio occurs when the TBM cutters break the rock mass into rock chips with larger size [21]. Meanwhile, invalid energy consumption occurs in the production of rock chips with smaller particle size (including the rock powder). The size of rock chips increases with the rise of rock-breaking efficiency of TBM; therefore, the proportion of larger size rock chips is a key indicator of TBM rock-breaking efficiency.

The shape and particle size distribution of rock chips are impacted by geological conditions, tunneling parameters, equipment parameters, and especially cutter spacing [13]. The rock chip information can comprehensively reflect the rock mass characteristics and the rock-breaking efficiency of TBM. In the Lanzhou water source construction project

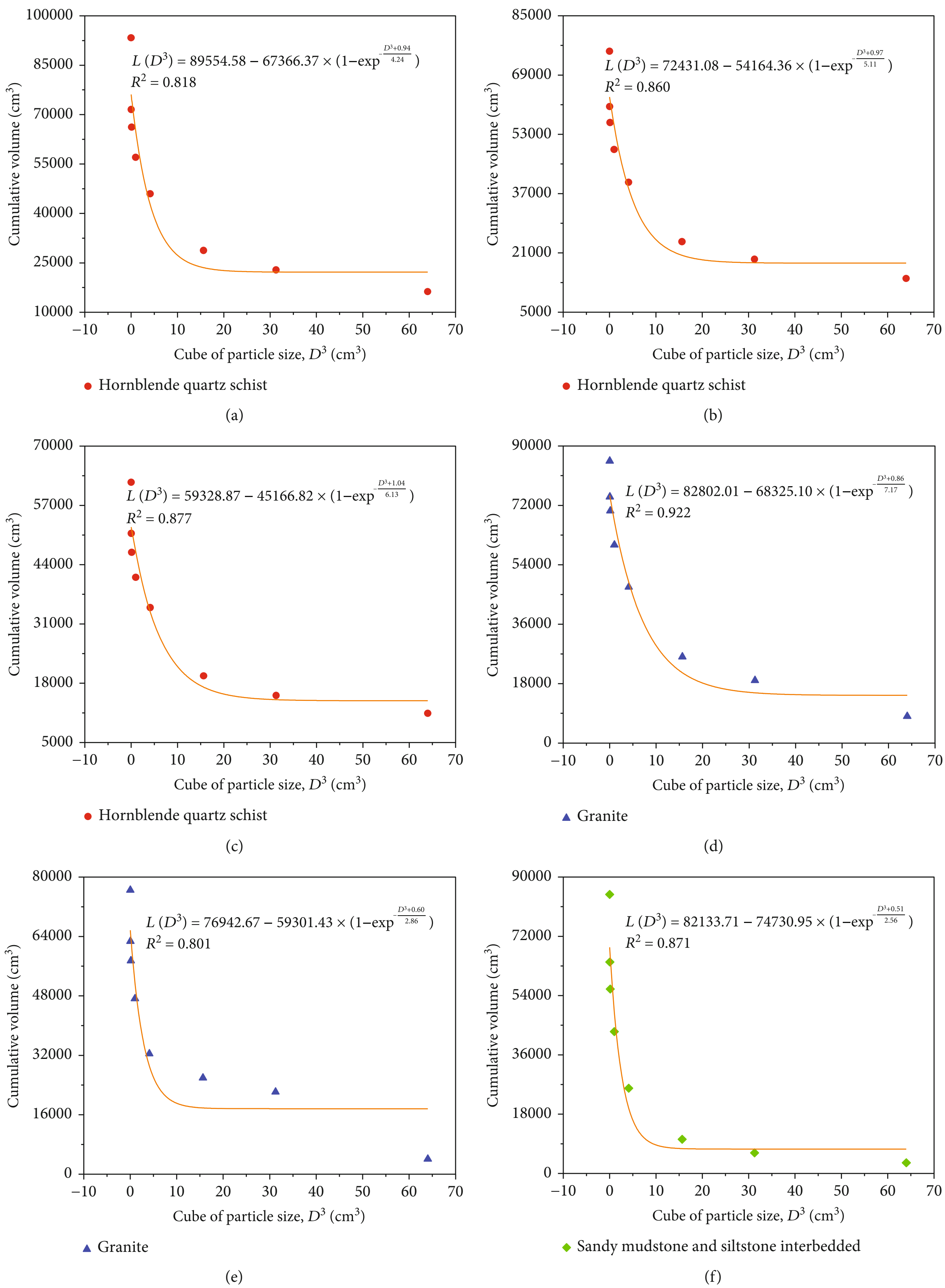

Figure 6: Continued.

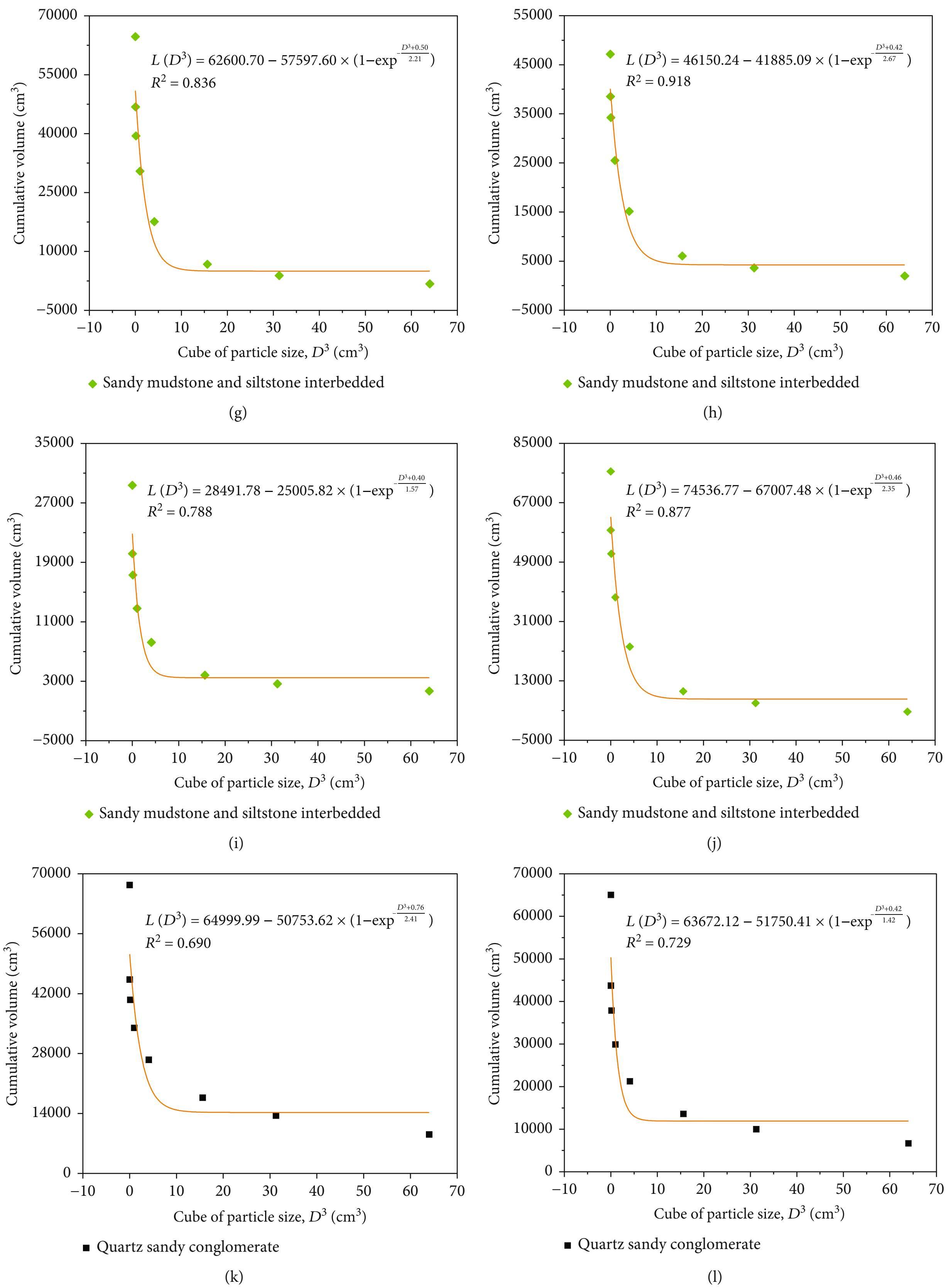

Figure 6: Rock chip cumulative volume distribution model for different groups: (a) group 1; (b) group 2; (c) group 3; (d) group 4; (e) group 5; (f) group 6; (g) group 7; (h) group 8; (i) group 9; (j) group 10; (k) group 11; (l) group 12.

Table 5: Ratios of major axis to medium axis and minor axis for different lithologies.

Lithology	j/q	j/t
Hornblende quartz schist	1.63	4.28
Granite	1.42	3.66
Sandy mudstone and siltstone interbedded	1.94	3.21
Quartz sandy conglomerate	1.77	6.43

and Wananxi water diversion project, the cutter spacing is generally between 30 and 100 mm, and the particle size of larger rock chips formed during TBM tunneling is generally between 5 and 70 mm.

A new evaluation index is in need that can accurately characterize the content of rock chips with larger size, comprehensively consider the rock chip information, and reasonably assess the rock-breaking efficiency of TBM. The effective rock-breaking ratio (P_r) is defined as follows:

$$P_r = \frac{\sum_{i=0.5}^{i=D_{max}} S_i}{S_T} \times 100\%, \quad (5)$$

where D_{max} represents the largest particle size of rock chips (cm) and $\sum_{i=0.5}^{i=D_{max}} S_i$ represents the total surface area of rock chips with particle size ≥ 0.5 cm (cm^2).

P_r is proposed based on the total surface area of rock chips; the shape, size, and particle size distribution of rock chips were comprehensively considered. Its calculated values are shown in Table 6. The P_r values of grade II surrounding rock range from 98.50 to 99.90, and that of grade III surrounding rock range from 98.57 to 99.40.

4. Rock-Breaking Efficiency Evaluation Indices of TBM

The previous rock-breaking efficiency evaluation indices (CI and SE) proposed were introduced in this section; the indices were mainly calculated based on indoor linear cutting machine test and field sieving test. The CI, SE, and P_r values of this study were calculated based on the field tunnel construction projects. The correlations among CI, SE, and P_r were analyzed.

4.1. Coarseness Index. The coarseness index [29] of rock chips is a common index to evaluate the rock-breaking efficiency of TBM and can be obtained by indoor linear cutting tests and TBM construction site [28, 38]. CI is calculated as follows:

$$X_i = \frac{W_i}{W_t} \times 100\%, \quad (6)$$

$$CI = \sum X_i, \quad (7)$$

where X_i represents the accumulated retained percentage of rock chips greater than a certain particle size, W_i represents the mass of rock chips larger than a certain particle size (kg), W_t represents the total mass of rock chips (kg), and CI is the coarseness index of rock chips.

The higher the rock-breaking efficiency of TBM, the more rock flakes and the less rock powder is produced by disc cutters breaking the rock, and the larger the CI, and vice versa [28, 38]. CI values (as shown in Table 6) were calculated based on the field sieving test results.

However, according to Eq. (6) and Eq. (7), CI value is obtained by adding the accumulated retained percentage of each aperture. The rock chips with larger particle size are repeatedly calculated; the larger the particle size, the more times the rock chip content is calculated.

4.2. Specific Energy. Specific energy is the mechanical work required to cut a unit volume of rock [7], which can directly measure the rock-breaking efficiency of TBM. The lower the SE value, the smaller the mechanical work is required to break a unit volume of rock, and the higher the rock-breaking efficiency of TBM. The calculation of SE [31] is expressed as follows:

$$SE = \frac{F_v l + M\theta}{l\pi R^2}, \quad (8)$$

where SE is the specific energy (MJ/m^3), F_v is the average thrust force of TBM (kN), l is the tunneling distance of TBM for a certain period (m), M is the average torque of TBM tunneling (kN·m), ⍰ is the rotation angle of the cutter (radian), and R is the radius of the excavated tunnel (m). The specific energy can be calculated by Eq. (8) as shown in Table 6.

SE is often calculated based on the average values of tunneling parameters. However, the thrust force, torque, and penetration of TBM vary greatly due to the influence of surrounding rock strength, integrity, and water content. Therefore, SE cannot be used to accurately evaluate excavation efficiency of TBM.

4.3. Correlation between CI and P_r. Both CI and P_r could reflect the fragmentation degree of rock chips; the more fragmentary the rock chips, the less the CI and P_r values. The linear regression analysis was used to investigate the correlation between the CI and P_r (as shown in Figure 7). Figure 7 shows that CI values increase with the rise of P_r values under both grade II and III surrounding rock conditions. The linear regression results suggest that the correlation between CI values and P_r values of grade II surrounding rock is statistically stronger than that of grade III surrounding rock, which is mainly ascribed to the poor integrity of grade III surrounding rock.

4.4. Correlation between SE and P_r. Both SE and P_r can reflect the rock-breaking efficiency of TBM; the higher the excavation efficiency of TBM, the less the SE value, the larger the P_r value. This study investigated the correlation between SE and P_r for grade II and III surrounding rocks (as shown in Figure 8). Figure 8 shows that SE values decrease with the rise of P_r values under both grade II and III surrounding rock conditions. The correlation between SE and P_r under

Table 6: Rock-breaking efficiency evaluation indices of TBM.

Group	Project	Lithology	Hardness	Integrity grade	Effective rock-breaking ratio (P_r, %)	Coarseness index (CI)	Specific energy (SE, MJ/m^3)	Thrust force (TF, kN)
1	Lanzhou TBM 1	Hornblende quartz schist	Hard	II	99.60	430.81	51.58	9000
2					99.71	448.88	32.22	8000
3					99.78	454.06	29.26	6500
4		Granite			99.81	429.67	46.15	8500
5					99.90	457.58	38.06	8000
6	Lanzhou TBM 2	Sandy mudstone and siltstone interbedded	Soft	III	98.57	326.74	29.87	4500
7					99.26	347.60	19.94	4000
8					99.18	328.00	27.40	4500
9					99.35	350.66	19.62	2500
10					99.40	366.00	17.36	1500
11	Wananxi TBM	Quartz sandy conglomerate	Hard	II	98.96	350.74	68.82	5000
12					98.50	377.28	78.51	5500

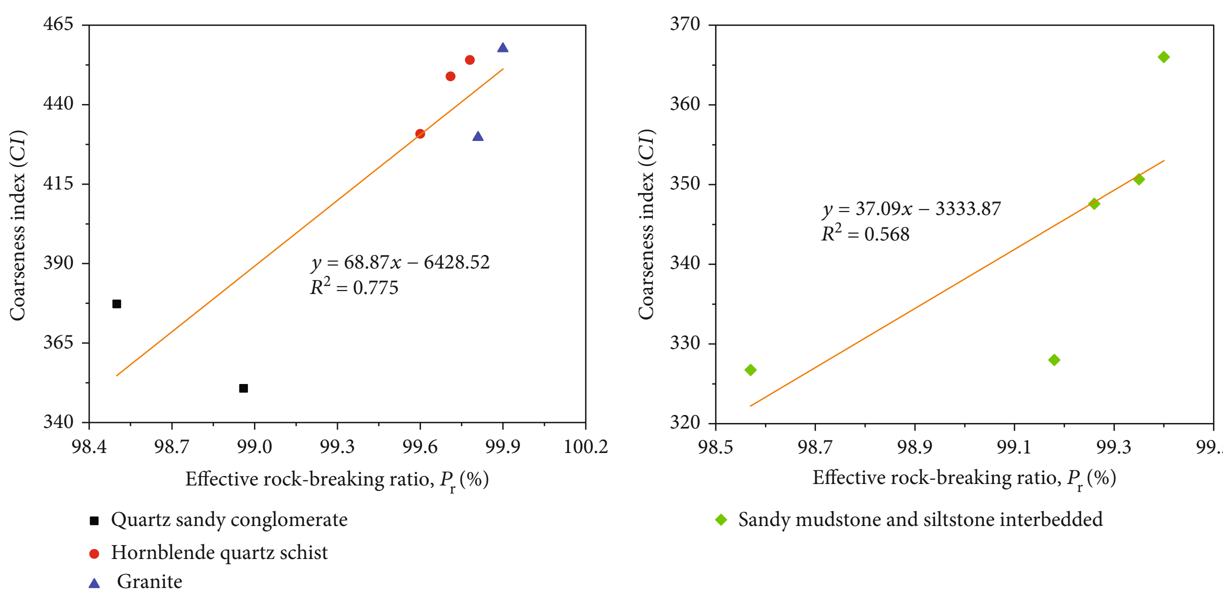

Figure 7: Correlation between CI and P_r.

grade II surrounding rock is more substantial than that under grade III surrounding rock, as suggested by the coefficient of determination (as shown in Figure 8), which is mainly due to the great varying range of tunneling parameters (such as thrust force, penetration, and torque) under grade III surrounding rock construction condition.

5. The Optimal Thrust Force Based on the P_r Index

The rock strength and hardness have certain influences on thrust force [38]. Thrust force has a significant impact on the rock-breaking efficiency of TBM and fragmentation degree of rock chips. Therefore, the determination of the optimal thrust force of TBM for different surrounding rocks is crucial for tunnel construction. Existing literature investigated how to determine the optimal thrust force based on laboratory or field rock-breaking experiments. Gong et al. [25] analyzed the TBM chipping efficiency under different cutter thrusts and obtained the critical value of cutter thrust. Yan et al. [38] suggested the optimal thrust force of different surrounding rocks based on the coarseness index. The thrust force data (as shown in Table 6) was collected from the Lanzhou water conveyance project and Wananxi water conveyance project. The regression models were developed to predict the optimal thrust force for grade II and III surrounding rocks (as shown in Eqs. (9) and (10)). Figure 9 shows that P_r increases at first and then decreases with the

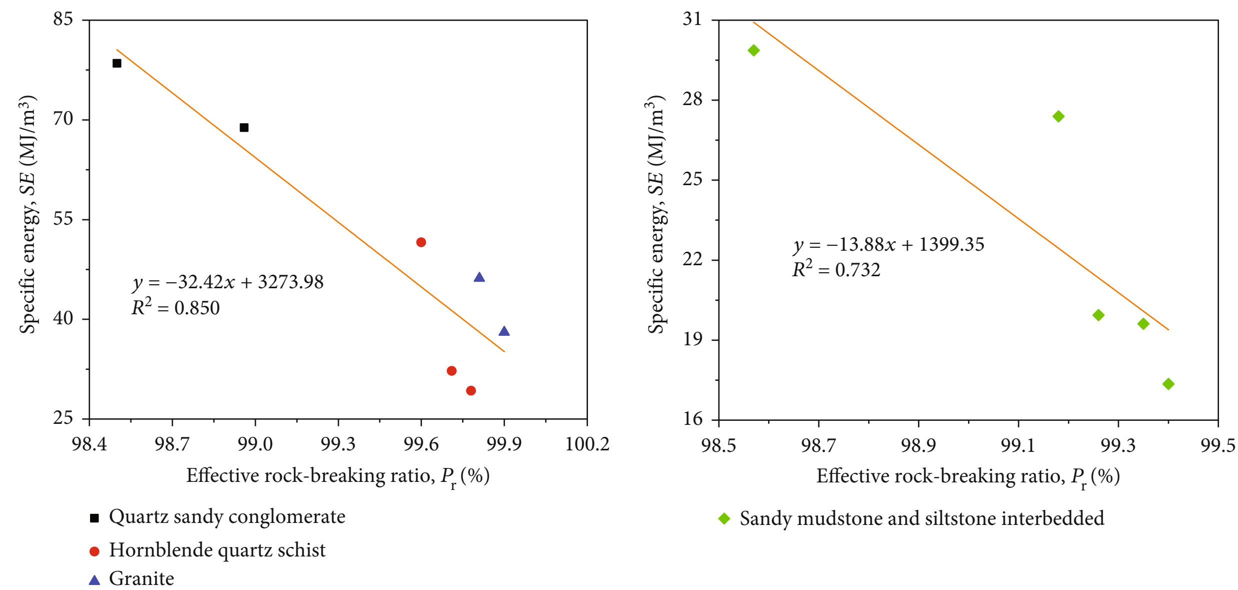

(a) Grade II surrounding rock

(b) Grade III surrounding rock

Figure 8: Correlation between SE and P_r.

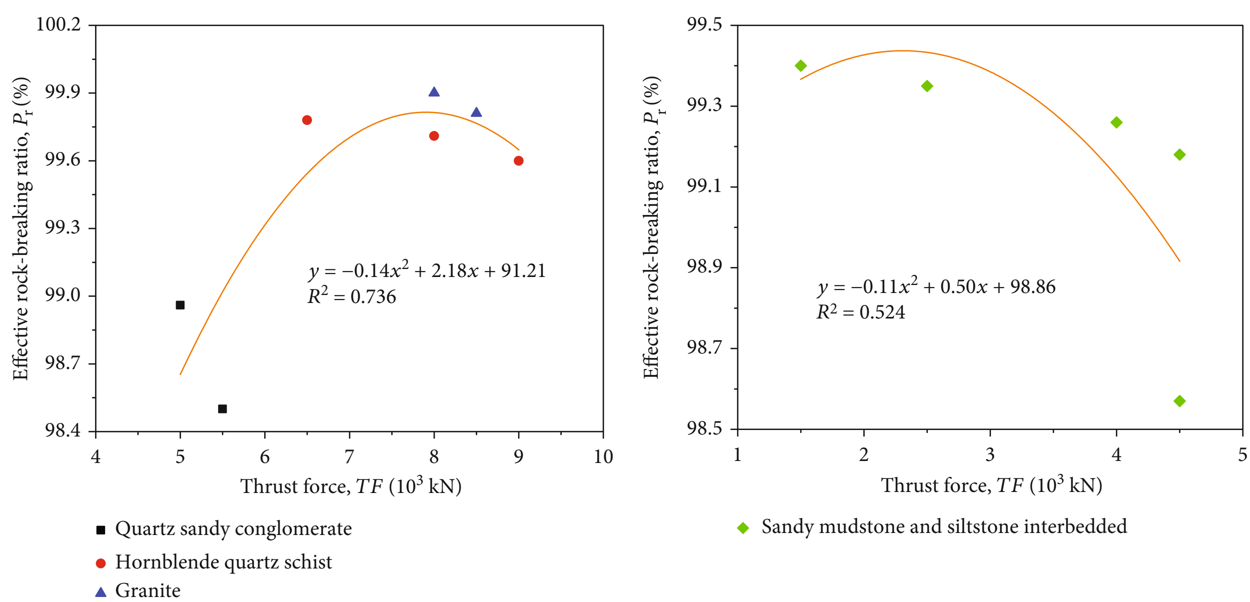

(a) Grade II surrounding rock

(b) Grade III surrounding rock

Figure 9: Correlation between P_r and thrust force.

rise of thrust force under different surrounding rock conditions. The correlation between P_r and thrust force of grade II surrounding rock is more substantial than that of grade III surrounding rock, which is mainly due to the poor integrity of grade III surrounding rock and large variable range of TBM tunneling parameters. The optimal thrust force intervals (i.e., the maximum P_r value) of the grade II and III surrounding rocks are about 7700-8000 kN and 2200-2400 kN, respectively, which could provide reasonable suggestions for engineers.

$$P_r = -0.14\mathrm{TF}^2 + 2.18\mathrm{TF} + 91.21 \quad \left(R^2 = 0.736\right), \tag{9}$$

$$P_r = -0.11\mathrm{TF}^2 + 0.50\mathrm{TF} + 98.86 \quad \left(R^2 = 0.524\right), \tag{10}$$

where TF represents the thrust force of TBM (10^3 kN).

6. Conclusions

This study proposed a novel index of effective rock-breaking ratio (P_r) for a more reasonable evaluation of the rock-breaking efficiency of TBM, which can comprehensively consider the rock chip information. The correlation among CI, SE, and P_r was analyzed, and the optimal thrust force was obtained using TBM excavation parameters from the in situ construction data. The main conclusions are shown as follows:

(1) Rock chip cumulative volume distribution model was developed to indirectly obtain the quantitative characteristic of rock chips. The surface area of rock chips could be calculated by the model. The novel TBM rock-breaking efficiency evaluation index (P_r) is obtained based on the surface area of rock chips, which generally considers the rock chip information

(2) P_r has a good linear correlation with CI and SE; the higher the TBM tunneling efficiency, the larger the P_r and CI values, the less the *SE* value

(3) P_r increases at first and then decreases with the rise of thrust force of TBM. The optimal thrust force intervals for grade II and III surrounding rocks can be determined to improve the rock-breaking efficiency of TBM

Abbreviations

TBM:	Tunnel boring machine
P_r:	Effective rock-breaking ratio (%)
CI:	Coarseness index
SE:	Specific energy (MJ/m^3)
$L(D^3)$:	The cumulative volume of rock chips larger than a certain particle size (cm^3)
D:	Particle size of rock chips (cm)
D^3:	Cube of rock chip particle size (cm^3)
S_i:	Surface area of a single particle (cm^2)
j:	Major axis of the ellipsoid (cm)
q:	Medium axis of the ellipsoid (cm)
t:	Minor axis of the ellipsoid (cm)
S_T:	Total surface area of rock chips (cm^2)
D_{max}:	The maximum medium axis of rock chips (cm)
$\sum_{i=0.5}^{i=D_{max}} S_i$:	The total surface area of rock chips with particle size ≥ 0.5 cm (cm^2)
X_i:	Accumulated retained percentage of rock chips greater than a certain particle size (%)
W_i:	Mass of rock chips larger than a certain particle size (kg)
W_t:	Total mass of rock chips (kg)
F_v:	Average thrust force of TBM (kN)
l:	Tunneling distance of TBM for a certain period of time (m)
M:	Average torque of TBM tunneling (kN·m)
θ:	Angle of cutter rotation (radian)
R:	Radius of the excavated tunnel (m)
TF:	Thrust force of TBM (10^3 kN).

Data Availability

The data that support the findings of this study are available from the corresponding author upon reasonable request.

Conflicts of Interest

The authors declare that they have no conflicts of interest.

Acknowledgments

This work was supported by the National Natural Science Foundation of China (41972270 and 42002281) and the Opening Foundation of State Key Laboratory of Shield Machine and Boring Technology (SKLST-2019-K06).

References

[1] G. Armetti, M. R. Migliazza, F. Ferrari, and P. Padovese, "Geological and mechanical rock mass conditions for TBM performance prediction. The case of "La Maddalena" exploratory tunnel, Chiomonte (Italy)," *Tunnelling and Underground Space Technology*, vol. 77, pp. 115–126, 2018.

[2] N. Barton, *TBM Tunnelling in Jointed and Faulted Rock*, Crc Press, 2000.

[3] A. Bruland, *Hard Rock Tunnel Boring, [Ph.D. Thesis]*, Norwegian university of science and technology, Trondheim, 1998.

[4] S. X. Feng, Z. Y. Chen, H. Luo et al., "Tunnel boring machines (TBM) performance prediction: a case study using big data and deep learning," *Tunnelling and Underground Space Technology*, vol. 110, article 103636, 2021.

[5] X. Huang, Q. S. Liu, K. Shi, Y. C. Pan, and J. P. Liu, "Application and prospect of hard rock TBM for deep roadway construction in coal mines," *Tunnelling and Underground Space Technology*, vol. 73, pp. 105–126, 2018.

[6] Q. S. Liu, X. Huang, Q. M. Gong, L. J. Du, Y. C. Pan, and J. P. Liu, "Application and development of hard rock TBM and its prospect in China," *Tunnelling and Underground Space Technology*, vol. 57, pp. 33–46, 2016.

[7] R. A. Snowdon, M. D. Ryley, and J. Temporal, "A study of disc cutting in selected British rocks," *International Journal of Rock Mechanics and Mining Science and Geomechanics Abstracts*, vol. 19, no. 3, pp. 107–121, 1982.

[8] D. L. Jin, D. J. Yuan, X. G. Li, and W. L. Su, "Probabilistic analysis of the disc cutter failure during TBM tunneling in hard rock," *Tunnelling and Underground Space Technology*, vol. 109, article 103744, 2021.

[9] H. Bejari and J. K. Hamidi, "Simultaneous effects of joint spacing and orientation on TBM cutting efficiency in jointed rock masses," *Rock Mechanics and Rock Engineering*, vol. 46, no. 4, pp. 897–907, 2013.

[10] S. H. Chang, S. W. Choi, G. J. Bae, and S. Jeon, "Performance prediction of TBM disc cutting on granitic rock by the linear cutting test," *Tunnelling and Underground Space Technology*, vol. 21, no. 3-4, p. 271, 2006.

[11] E. Farrokh and J. Rostami, "Correlation of tunnel convergence with TBM operational parameters and chip size in the Ghomroud tunnel, Iran," *Tunnelling and Underground Space Technology*, vol. 23, no. 6, pp. 700–710, 2008.

[12] Q. M. Gong and J. Zhao, "Development of a rock mass characteristics model for TBM penetration rate prediction," *International Journal of Rock Mechanics and Mining Sciences*, vol. 46, no. 1, pp. 8–18, 2009.

[13] D. Y. Han, P. Cao, J. Liu, and J. B. Zhu, "An experimental study of dependence of optimum TBM cutter spacing on pre-set

penetration depth in sandstone fragmentation," *Rock Mechanics and Rock Engineering*, vol. 50, no. 12, pp. 3209–3221, 2017.

[14] S. Heydari, J. K. Hamidi, M. Monjezi, and A. Eftekhari, "An investigation of the relationship between muck geometry, TBM performance, and operational parameters: a case study in Golab II water transfer tunnel," *Tunnelling and Underground Space Technology*, vol. 88, pp. 73–86, 2019.

[15] F. S. Miao, Y. P. Wu, Y. H. Xie, and Y. N. Li, "Prediction of landslide displacement with step-like behavior based on multialgorithm optimization and a support vector regression model," *Landslides*, vol. 15, no. 3, pp. 475–488, 2018.

[16] F. S. Miao, Y. P. Wu, Á. Török, L. W. Li, and Y. Xue, "Centrifugal model test on a riverine landslide in the Three Gorges Reservoir induced by rainfall and water level fluctuation," *Geoscience Frontiers*, vol. 13, no. 3, article 101378, 2022.

[17] T. Moon and J. Oh, "A study of optimal rock-cutting conditions for hard rock TBM using the discrete element method," *Rock Mechanics and Rock Engineering*, vol. 45, no. 5, pp. 837–849, 2011.

[18] Y. C. Pan, Q. S. Liu, J. P. Liu, X. X. Kong, X. X. Peng, and Q. Liu, "Investigation on disc cutter behaviors in cutting rocks of different strengths and reverse estimation of rock strengths from experimental cutting forces," *European Journal of Environmental and Civil Engineering*, vol. 25, no. 1, pp. 1–27, 2021.

[19] Y. C. Pan, Q. S. Liu, J. P. Liu, Q. Liu, and X. X. Kong, "Full-scale linear cutting tests in Chongqing sandstone to study the influence of confining stress on rock cutting efficiency by TBM disc cutter," *Tunnelling and Underground Space Technology*, vol. 80, pp. 197–210, 2018.

[20] Z. J. Wu, P. L. Zhang, L. F. Fan, and Q. S. Liu, "Numerical study of the effect of confining pressure on the rock breakage efficiency and fragment size distribution of a TBM cutter using a coupled FEM- DEM method," *Tunnelling and Underground Space Technology*, vol. 88, pp. 260–275, 2019.

[21] X. H. Xu and J. Yu, *Rock Fragment*, China Coal Industry Publishing House, Beijing, 1984.

[22] J. Rostami and L. Ozdemir, "A new model for performance prediction of hard rock TBM," in *Proceedings of RETC*, pp. 793–809, Boston, MA, 1993.

[23] X. H. Zhang, D. B. Hu, J. M. Li, J. J. Pan, Y. M. Xia, and Y. C. Tian, "Investigation of rock breaking mechanism with TBM hob under traditional and free-face condition," *Engineering Fracture Mechanics*, vol. 242, article 107432, 2021.

[24] A. Rispoli, A. M. Ferrero, M. Cardu, and A. Farinetti, "Determining the particle size of debris from a tunnel boring machine through photographic analysis and comparison between excavation performance and rock mass properties," *Rock Mechanics and Rock Engineering*, vol. 50, no. 10, pp. 2805–2816, 2017.

[25] Q. M. Gong, J. Zhao, and Y. S. Jiang, "In situ TBM penetration tests and rock mass boreability analysis in hard rock tunnels," *Tunnelling and Underground Space Technology*, vol. 22, no. 3, pp. 303–316, 2007.

[26] A. Shaterpour-Mamaghani and N. Bilgin, "Some contributions on the estimation of performance and operational parameters of raise borers - a case study in Kure Copper Mine, Turkey," *Tunnelling and Underground Space Technology*, vol. 54, pp. 37–48, 2016.

[27] H. Tuncdemir, N. Bilgin, H. Copur, and C. Balci, "Control of rock cutting efficiency by muck size," *International Journal of Rock Mechanics and Mining Sciences*, vol. 45, no. 2, pp. 278–288, 2008.

[28] Q. M. Gong, X. X. Zhou, L. J. Yin, G. W. He, and C. T. Miao, "Study of rock breaking efficiency of TBM disc cutter based on chips analysis of linear cutting test," *Tunnel Construction*, vol. 37, no. 3, pp. 363–368, 2017.

[29] F. F. Roxborough and A. Rispin, "The mechanical cutting characteristics of the lower chalk," *Tunnels & Tunnelling International*, vol. 5, no. 3, pp. 45–67, 1973.

[30] O. Acaroglu, L. Ozdemir, and B. Asbury, "A fuzzy logic model to predict specific energy requirement for TBM performance prediction," *Tunnelling and Underground Space Technology*, vol. 23, no. 5, pp. 600–608, 2008.

[31] L. H. Wang, Y. L. Kang, Z. X. Cai et al., "The energy method to predict disc cutter wear extent for hard rock TBMs," *Tunnelling and Underground Space Technology*, vol. 28, pp. 183–191, 2012.

[32] M. Mohammadi, J. K. Hamidi, J. Rostami, and K. Goshtasbi, "A closer look into chip shape/size and efficiency of rock cutting with a simple chisel pick: a laboratory scale investigation," *Rock Mechanics and Rock Engineering*, vol. 53, no. 3, pp. 1375–1392, 2020.

[33] R. Kumar, V. M. S. R. Murthy, and L. A. Kumaraswamidhas, "Performance analysis of rotary blast-hole drills through machine vibration and coarseness index mapping - a novel approach," *Measurement*, vol. 165, article 108148, 2020.

[34] J. W. Cho, S. Jeon, H. Y. Jeong, and S. H. Chang, "Evaluation of cutting efficiency during TBM disc cutter excavation within a Korean granitic rock using linear-cutting-machine testing and photogrammetric measurement," *Tunnelling and Underground Space Technology*, vol. 35, pp. 37–54, 2013.

[35] The National Standards Compilation Group of People's Republic of China, *GB 50487-2008 Code for Engineering Geological Investigation of Water Resources and Hydropower*, China Planning Press, Beijing, 2009.

[36] The National Standards Compilation Group of People's Republic of China, *GB/T 50218-2014 Standard for Engineering Classification of Rock Masses*, China Planning Press, Beijing, 2015.

[37] W. L. Chen, K. Fukui, and S. Okubo, "Study on the detritus from different excavation machines and methods," *Chinese Journal of Rock Mechanics and Engineering*, vol. 22, no. 6, pp. 1037–1043, 2003.

[38] C. B. Yan, X. D. Jiang, Z. H. Liu, J. H. Yang, and D. Miao, "Rock-breaking efficiency of TBM based on particle-size distribution of rock detritus," *Chinese Journal of Geotechnical Engineering*, vol. 41, no. 3, pp. 466–474, 2019.

[39] K. Z. Song, L. G. Ji, and D. J. Yuan, "Research on distribution regularities of grain size of rock detritus from discoid cutters," *Chinese Journal of Rock Mechanics and Engineering*, vol. 27, no. S1, pp. 3016–3022, 2008.